Available online at www.sciencedirect.com

ScienceDirect

IFAC PapersOnline CONFERENCE PAPER ARCHIVE

IFAC PapersOnLine 58-28 (2024) 816–821

Co-Design for Real-Time Adaptability: Methodology and Wind Energy Case Study ⋆

Jacob B. Fine * **Ian Holbrook** * **Chris Vermillion** *

* *University of Michigan, Ann Arbor, MI USA (e-mail: jbfine@umich.edu).*

Abstract:
This work presents a unique control co-design formulation that explicitly optimizes the level of real-time adaptability in both the physical design and control parameters. Adaptability is particularly important for large-scale energy-harvesting systems, which operate in highly variable environments and are subject to long design and manufacturing cycles. Here, physical components and software often must be "frozen" relatively early, sometimes well-before the system's dynamics have been fully characterized. The proposed co-design framework performs a maximization of expected profit, accounting for a low-complexity surrogate model of the system's performance, a statistical model of the environment, a statistical characterization of how modeling uncertainty diminishes over the design cycle, and cost models that consider the price of adaptability. This co-design framework is coupled with an online control strategy that performs the real-time adaptation, subject to constraints. To evaluate this approach, we focus on the segmented ultralight morphing rotor (SUMR) described in Noyes et al. (2020), Zalkind et al. (2017), Kianbakht et al. (2022), and Ananda et al. (2018). Applying the co-design framework to the SUMR, and utilizing the aforementioned performance surrogate model, the expected lifetime profit is shown to increase by 6.5% when the level of adaptability is optimized. Over a 24-hour dynamic simulation, the predictions based on the simplified surrogate model are shown to deviate by less than 1% relative to the results of the higher-fidelity dynamic model (which is suitable for 24-hour simulations but not for long-term profitability projections).

Keywords: Hardware/software co-design, Energy systems, Control of renewable energy resources, Optimal operation and control of power systems, adaptive control

1. INTRODUCTION

In the face of the escalating global climate crisis, there is a pressing need for energy solutions that are both environmentally sustainable and economically viable. Projections indicate that within the next three decades, the United States is anticipated to double its capacity for renewable energy production, constituting 42% of the nation's total power generation (Holtberg et al. (2011)). Fulfilling the demand for sustainable energy necessitates the development of economically feasible renewable energy systems. Wind energy emerges prominently as a substantial renewable resource worldwide. Remarkable advancements in wind energy technology over the past decade have enabled it to provide power at costs comparable to (or even lower than) fossil fuels in numerous regions. Wind energy installations have accounted for 28% of the United States' capacity expansions in the preceding decade (Wiser and Bolinger (2019)).

While the prevalence of wind power has increased drastically over the last decade, economic optimization of these systems (and renewable energy systems as a whole) is made particularly challenging for at least two reasons. First, the optimal plant and controller parameters depend strongly on both the environmental energy resource and each other as described in Pao et al. (2023). To deal with this uncertainty, several works such as Pao et al. (2023), Bayat et al. (2023), and Naik and Vermillion (2024) have presented co-design methodologies for considering this coupling in tandem with a stochastic energy resource. Secondly, as indicated in Roberto Lacal-Arántegui (2018), the development of renewable energy systems is subject to long design cycles with design freeze dates that often come before either the device's dynamical behavior or the environmental resource (ascertained via site studies) have been fully quantified.

One mechanism for improving the performance of an energy system in the presence of modeling and environmental uncertainty is to incorporate real-time controller and plant adaptability. Physical adaptability of energy-harvesting kites has been studied in the context of both chord and span morphing in Fine et al. (2022) and Fine et al. (2023). Additionally, a large body of literature has demonstrated that significant performance gains can be realized through real-time controller adaptation (e.g. Rotea (2017)). If a system is designed with adaptive plant and controller parameters, the system can be reconfigured after the plant and controller freeze dates. However, adaptability comes at a cost, either in the form of a more complex physical design or additional software development. While these benefits and challenges with adaptability are generally well-understood, no co-design formulation to-date has provided a quantitative framework for optimizing adaptability.

We present a formal co-design formulation that treats the levels of plant and controller adaptability as decision variables. Central to the work is the concept of an "adaptability set". The size of a system's adaptability set dictates how much plant and controller parameters can be varied during operation. To optimize the dimensions of this set, it is necessary to quantitatively

⋆ This research was supported by the National Science Foundation Award Number 2321698.

10.1016/j.ifacol.2025.01.076

understand the expected costs and benefits of adaptability in the presence of a stochastic environment and evolving (decreasing in time) modeling uncertainty. To accomplish this, the proposed co-design formulation relies on several ingredients to maximize the expected lifetime profit of an energy device in the presence of adaptability. Those components include (i) a low-complexity surrogate model of the system's performance, (ii) a statistical model of the environment, (iii) a statistical characterization of how modeling uncertainty diminishes over the design cycle, and (iv) cost models that quantify the price of adaptability (in terms of additional mechanical hardware and/or software development). To realize real-time plant and controller adaptation, we rely on a combination of a wind-driven lookup table coupled with a simple feedback controller.

To demonstrate the efficacy of this framework, we performed a case study on the Segmented Ultralight Morphing Rotor (SUMR). The SUMR was analyzed in this work because the system is both well-characterized (dynamically and economically) and capable of real-time plant adaptation (see Noyes et al. (2020), Zalkind et al. (2017), Kianbakht et al. (2022), and Ananda et al. (2018)). Like a palm tree in the wind, the SUMR turbine can increase the coning angle of the blades (folding the blades inwards) in response to high wind speeds, reducing structural loading on the blade roots significantly, providing an efficient mechanism for curtailment to a structural limitation and allowing the turbine to operate at high wind speeds. A system model of the SUMR wind turbine (from Zalkind et al. (2017)) is shown in Fig. 1. Our results show a 6.5% projected increase in lifetime profitability based on our surrogate model for optimization. Furthermore, 24-hour simulations on a higher-fidelity dynamic model show less than 1% difference from the surrogate model.

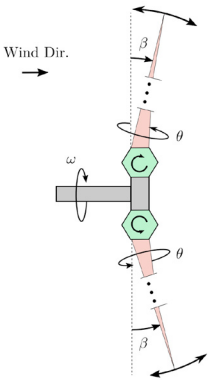

Fig. 1. System Model of the SUMR from Zalkind et al. (2017) (used with permission). In this diagram, ω represents the turbine's angular velocity, β represents the blade coning angle, and θ represents the blade pitch angle.

2. CO-DESIGN FORMULATION

Our ultimate objective is to maximize the expected lifetime profit. Accounting for modeling and environmental uncertainty, the expected power generated is given by:

$$\hat{P}_{\text{avg}} = \int_{z_{\text{mdl,min}}}^{z_{\text{mdl,max}}} \int_{z_{\text{env,min}}}^{z_{\text{env,max}}} \rho_{\text{mdl}}(z_{\text{mdl}}|\boldsymbol{t}_p,\boldsymbol{t}_c)\rho_{\text{env}}(z_{\text{env}}) \hat{P}^*(z_{\text{env}},\boldsymbol{A}_p,\boldsymbol{A}_c,z_{\text{mdl}})dz_{\text{env}}dz_{\text{mdl}} \tag{1}$$

where

$$\hat{P}^*(z_{\text{env}},\boldsymbol{A}_p,\boldsymbol{A}_c,z_{\text{mdl}}) = \max_{\boldsymbol{x}_p\in\boldsymbol{A}_p,\boldsymbol{x}_c\in\boldsymbol{A}_c} \hat{P}(z_{\text{env}},\boldsymbol{x}_p,\boldsymbol{x}_c,z_{\text{mdl}}) \tag{2}$$

Here, $\hat{P}_{\text{avg}}$ is the estimated average power generated by the candidate system design, ρ_{env} is the probability density function (PDF) of the environmental energy resource z_{env} (evaluated between $z_{\text{env,min}}$ and $z_{\text{env,max}}$), ρ_{mdl} is the PDF of uncertain model parameters z_{mdl} (evaluated between $z_{\text{mdl,min}}$ and $z_{\text{mdl,max}}$), $\hat{P}$ is the predicted power generation, $\hat{P}^*$ is the predicted maximal achievable power generation at a single environmental condition and level of model uncertainty for any plant and controller design contained within the "adaptability sets" $\boldsymbol{A}_p$ and $\boldsymbol{A}_c$. These sets, which are hypervolumes within the space of admissible plant and controller designs ($\boldsymbol{x}_p$ and $\boldsymbol{x}_c$), define the amount of real-time adaptation in plant and control variables (respectively) that is built into the design. When certain plant and control parameters are fixed (non-adaptive), $\boldsymbol{A}_p$ and $\boldsymbol{A}_c$ degenerate into lower-dimensional sets. Thus, without loss of generality, the full design, regardless of the amount (or existence) of adaptability, can be specified based on $\boldsymbol{A}_p$ and $\boldsymbol{A}_c$. The variables $\boldsymbol{t}_p$ and $\boldsymbol{t}_c$ are design freeze dates for the plant and controller, respectively. Because modeling uncertainty decays with time, the uncertainty present at the time of design finalization depends on these freeze dates; hence, the dependency in the PDF.

Given the objective of maximizing expected lifetime profit, it is necessary to model the system cost as a function of these same parameters. The overall cost of a system (K_{sys}) is calculated in Eqn. 3 and is composed of four components: K_{init} (the cost of the baseline design), K_{adapt} (the cost of incorporating a specified level of adaptability into the design), K_{time} (the cost of pushing back design freeze dates), and $K_{\text{O\&M}}$ (the cumulative cost of operation and maintenance).

$$\begin{aligned} K_{\text{sys}} = {} & K_{\text{init}}(\boldsymbol{A}_p,\boldsymbol{A}_c) + K_{\text{adapt}}(\boldsymbol{A}_p,\boldsymbol{A}_c) + K_{\text{time}}(\boldsymbol{t}_p,\boldsymbol{t}_c) \\ & + K_{\text{O\&M}}(\boldsymbol{A}_p,\boldsymbol{A}_c,L_{\text{sys}}(\boldsymbol{A}_p,\boldsymbol{A}_c),z_{\text{env}}) \end{aligned} \tag{3}$$

Given an economic value for energy (E_{val}) and an estimate of the system's expected lifetime (L_{sys}), the expected lifetime profit of an energy system can be expressed as:

$$J(\boldsymbol{A}_p,\boldsymbol{A}_c,\boldsymbol{t}_p,\boldsymbol{t}_c) = \hat{P}_{\text{avg}} L_{\text{sys}} E_{\text{val}} - K_{\text{sys}} \tag{4}$$

This expression, which has units of monetary currency, can also be divided by $\hat{P}_{\text{avg}} L_{\text{sys}}$ to obtain a metric that is equivalent to E_{val} minus the inverse of the familiar levelized cost of energy (LCOE). Thus, given a fixed value of E_{val}, the economic profitability metric in this work varies monotonically with LCOE.

While the co-design formulation is predicated on the three seemingly simple equations referenced in this section, the calculation of the constituent quantities requires significant effort. To ground this effort in an established application, we turn to the SUMR wind turbine in the following section.

3. THE SUMR TURBINE: AN IDEAL CASE STUDY

3.1 Background on the SUMR Turbine

The SUMR wind turbine is a two-bladed downwind turbine platform designed to enable the use of ultra-long blades through active coning (see Noyes et al. (2020) and Ananda et al. (2018)). By coning at high wind speeds, the SUMR reduces blade bending loads. Furthermore, variable coning functionality can be used to maximize power output in low-wind conditions, demonstrated in Noyes et al. (2020). Combined, these attributes enable the SUMR platform to

operate in a wider range of conditions and at rated power output more often than traditional turbines.

In this case study, the blade length (r_b) represents a non-adaptable plant decision variable, whereas the coning angle (β) is treated as adaptable, with a (to-be-optimized) margin of adaptability given by Δ_β. Thus, the plant adaptability set $\boldsymbol{A}_p$ is a line of length Δ_β. For the controller, we consider the possibility of having either a fixed or adaptive tip speed ratio (TSR) setpoint (where the adaptive TSR setpoint can be utilized to reduce loading in real time). This binary control-strategy decision variable is given by K_{type}. Thus, the controller adaptability set $\boldsymbol{A}_c$ is either a line spanning the full range of candidate TSR setpoints (when $K_{\text{type}}=1$) or a point (when $K_{\text{type}}=0$). Finally, the plant and controller freeze dates are given by t_p and t_c, respectively.

3.2 System Modeling

In this subsection, specific models for power generation, model uncertainty, and cost of the SUMR turbine are introduced. Specifically, the blade profile of the SUMR-13i, as described in Ananda et al. (2018), is considered. Additionally, a first-order dynamic model of the SUMR is introduced.

Aerodynamic Modeling: Using blade-element-momentum theory as described in P. J. Moriarty (2005), the coefficients of thrust (C_t) and power (C_p) were identified as functions of blade length, TSR, coning angle, and blade pitch (θ) based on the blade profile of the SUMR-13i as described in Ananda et al. (2018). This analysis also identified the aerodynamic torque (τ_{aero}) as a function of the same variables and wind speed. Using a control algorithm described in the following subsections, the blade pitch angle is modulated to curtail performance at high wind speeds to reduce the structural loading.

Quasi-static Performance Model: To reduce the computational complexity in computing P_{avg} (which already requires integration over a joint distribution of environmental and model uncertainty), a quasi-static expression for the average power generated by the SUMR turbine was defined as follows:

$$P_{\text{avg}}=\int_{\Delta_{\text{Cp,min}}}^{\Delta_{\text{Cp,max}}}\int_{v_{\text{w,min}}}^{v_{\text{w,max}}}\rho_{\text{mdl}}(\Delta_{\text{Cp}})\rho_{\text{env}}(v_w)\frac{1}{2}\rho_{\text{air}}\pi(r_b\cos\beta)^2 \Delta_{\text{Cp}}C_p(r_b,TSR,\beta,\theta)v_w^3 dv_w d\Delta_{\text{Cp}} \tag{5}$$

Here, v_w is the wind speed, ρ_{air} is the air density, and Δ_{Cp} represents a multiplicative uncertainty on the power coefficient. Furthermore, $\Delta_{\text{Cp,min}}$, $\Delta_{\text{Cp,max}}$, $v_{\text{w,min}}$, and $v_{\text{w,max}}$ describe the minimum and maximum values of Δ_{Cp} and v_w respectively. We seek to maximize this average power, subject to the allowable range of inputs, a structural constraint on the maximum allowable moment acting on the blade root, and a limit on the power generated by the turbine (the system's rated power). This results in the following optimization problem:

$$\max_{TSR,\beta,\theta} P_{\text{avg}}(v_w,r_b,\Delta_{\text{Cp}}) \tag{6}$$

subject to:

$$TSR\begin{cases}=TSR_{\text{nom}} & K_{\text{type}}=0\\ \in[TSR_{\text{min}},TSR_{\text{max}}] & K_{\text{type}}=1\end{cases} \tag{7}$$

$$\max(\beta_{\text{min}},\beta_{\text{nom}}-\Delta_\beta)\le\beta\le\min(\beta_{\text{max}},\beta_{\text{nom}}+\Delta_\beta) \tag{8}$$

$$\theta_{\text{min}}\le\theta\le\theta_{\text{max}} \tag{9}$$

$$M_{\text{root}}(v_w,r_b,TSR,\beta,\theta,\Delta_{\text{Cp}})\le M_{\text{max}} \tag{10}$$

$$P\le P_{\text{rated}} \tag{11}$$

where TSR_{min} and TSR_{max} refer to the minimum and maximum allowable tip-speed-ratio, TSR_{nom} refers to the nominal TSR setpoint if a non-adaptive controller is selected ($K_{\text{type}}=0$), β_{min} and β_{max} refer to the minimum and maximum allowable cone angle, β_{nom} refers to the nominal cone angle of the system, θ_{min} and θ_{max} refer to the minimum and maximum allowable blade pitch angle, M_{root} refers to the root bending moment, M_{max} refers to the maximum allowable bending moment, and P_{rated} refers to the turbine's rated power. Finally, the root bending moment was calculated as follows:

$$M_{\text{root}}=\frac{1}{4}\rho_{\text{air}}\pi(r_b\cos\beta)^2(1+a\Delta_{\text{Cp}}-a) C_t(r_b,TSR,\beta,\theta)v_w^2 y_{ac} \tag{12}$$

where y_{ac} is the spanwise location of the aerodynamic center of the blade, defined as $y_{ac}=r_b\frac{2^{2/3}}{2}$ based on a quadratic lift distribution, and a is the turbine's axial induction factor. The baseline design parameters of this system are listed in Table 1. Using this model, the average power generated by the SUMR is calculated as a function of the co-design decision variables.

Table 1. SUMR turbine baseline design parameters and constraints

Variable	Description	Value	Units
β_{nom}	Nominal cone angle	12.5	°
β_{min}	Minimum cone angle	0	°
β_{max}	Maximum cone angle	45	°
θ_{min}	Minimum pitch angle	0	°
θ_{max}	Maximum pitch angle	14	°
TSR_{min}	Minimum TSR	6	(-)
TSR_{max}	Maximum TSR	10	(-)
P_{rated}	Rated power	13.2	MW
M_{max}	Maximum root bending moment	50	MNm
ρ_{air}	Air Density	1.225	$\frac{kg}{m^3}$
a	Axial induction factor	0.333	(-)

Model Uncertainty: To perform the co-design optimization of the SUMR, it is necessary to understand how model uncertainty will evolve with time. The modeling uncertainty PDF is defined as:

$$\rho_{\text{mdl}}(\Delta_{C_P}|\boldsymbol{t}_p,\boldsymbol{t}_c)=\mathcal{N}(1,u(\boldsymbol{t}_p,\boldsymbol{t}_c)) \tag{13}$$

where u is the standard deviation in model uncertainty, which changes as a function of the plant and controller freeze dates. The specific profile for the evolution of uncertainty in this case study is shown in Fig. 2, reflecting an order of magnitude reduction in uncertainty over six months.

Environmental Model: Lansing, Michigan was identified as a candidate installation site. Here, surface wind speed measurements were available at 10-minute intervals via the National Solar Radiance Database (Sengupta et al. (2018)). A Weibull distribution was fit to this data at this site over a month to serve as the energy resource PDF (ρ_{PDF}), as shown in Fig. 3.

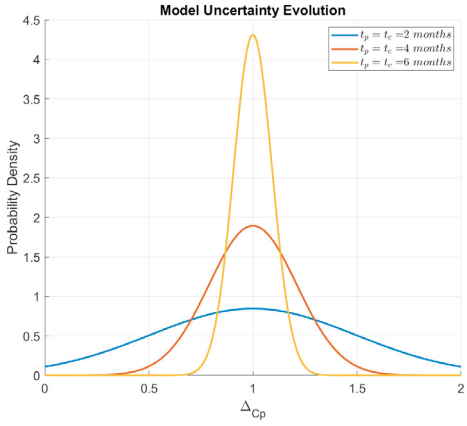

Fig. 2. The model uncertainty PDF at multiple freeze dates.

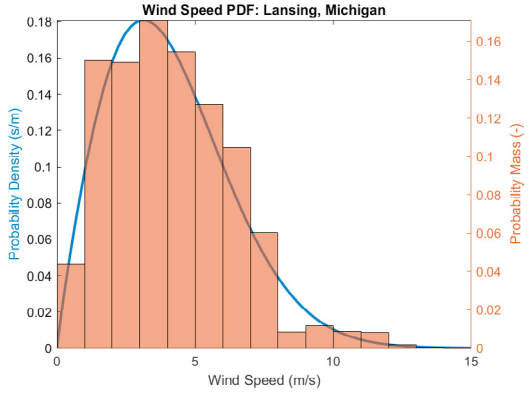

Fig. 3. Wind speed Weibull distribution and histogram.

System Cost Model: To maximize the lifetime profit of the SUMR turbine, it was first necessary to model system cost as a function of the co-design decision variables. The cost of the baseline design (K_{init}) was defined as a function of the blade mass. The approximate cost per unit of blade mass was defined in L. Fingersh and Laxson (2006). Leveraging the analysis described in Noyes et al. (2020), blade mass was obtained as a function of blade length. Using this, along with the knowledge that the blades comprise roughly 8% of the total cost of the SUMR (Noyes et al. (2020)), an approximate model of the total cost of the SUMR as a function of blade length was constructed as follows:

$$K_{\text{init}} = f_{\text{m,b}}(r_b) 15.62 \frac{\$}{kg} \tag{14}$$

where $f_{\text{m,b}}$ is an interpolation of the turbine mass as a function of length from the values provided in Noyes et al. (2020). Note that the TSR setpoint, which only needs to be selected at the design freeze date if a non-adaptive controller is selected ($K_{\text{type}} = 0$), does not impact the baseline cost of the system, as it is simply a parameter in the software.

To characterize the cost of the adaptive parameters (K_{adapt}), the hardware cost of integrating blade coning was estimated based on existing hardware cost models for adjustable blade pitch as described in L. Fingersh and Laxson (2006). To model the software development cost of real-time TSR adaptation (corresponding to $K_{\text{type}} = 1$), it was assumed that development of this controller would require one month of work from ten engineers (each compensated \$100/hour, including overhead). The net cost of adaptive parameters is described as follows:

$$K_{\text{adapt}} = f_{\text{m},\theta}(\Delta_\beta, f_{\text{m,b}}(r_b)) 15.62 \frac{\$}{kg} + \$250{,}000 K_{\text{type}} \tag{15}$$

where $f_{\text{m},\theta}$ is the mass of the blade pitch mechanism as described in L. Fingersh and Laxson (2006).

Additionally, the cost of the delaying freeze dates (K_{time}) needed to be characterized. For this case study, the cost of delaying the plant and controller freeze dates is calculated as follows under the practical assumption that the controller freeze date must occur on or after the plant freeze date.

$$K_{\text{time}} = 20000 \frac{\$}{month^2} (3\mathbf{t}_p^2 + \mathbf{t}_c^2) \tag{16}$$

Operation and maintenance costs were defined as a function of system capacity as described in Lantz et al. (2016) as:

$$K_{\text{O\&M}} = L_{\text{sys}} P_{\text{rated}} 35 \frac{\$}{kW year} \tag{17}$$

3.3 SUMR Turbine Adaptive Co-Design Results:

Combining the aforementioned models of performance, the environment, uncertainty, and cost, only two components remain unaccounted for in the objective described in Eqn. 4: the economic value of energy generated (E_{val}) and the expected lifetime of the system (L_{sys}). Assuming a saturated energy market and a relatively short system lifespan, these values were selected to be $0.10 \frac{\$}{kWh}$ and 30 years, respectively. Using these values, the objective surface in the absence of modeling uncertainty and adaption was plotted in Fig. 4. Note that, in the absence of plant and controller adaptability and with a perfect model of the system, the maximal achievable lifetime profit for the system was \$13.94MM.

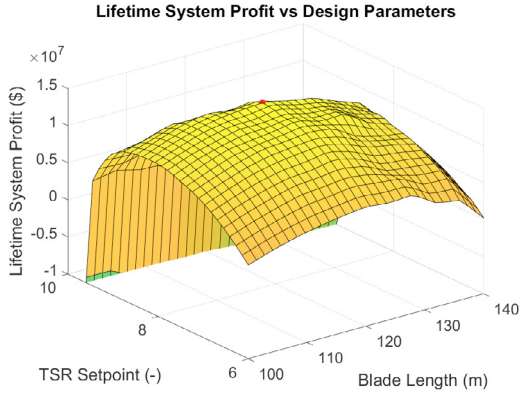

Fig. 4. True objective surface without adaptation.

The outlined co-design optimization was implemented in a nested formulation, wherein the optimal fixed design parameters were computed for every candidate combination of adaptability set size, plant freeze date, and controller freeze date. The expected lifetime system profit is plotted as a function of freeze dates, for multiple levels of adaptability, in Fig. 5. In this figure, the optimal freeze date for each level of adaptability (indicated by mesh color) is marked with an X on each surface. Systems designed with less adaptability tended to have later optimal freeze dates than those with more adaptability. This result can be attributed to the fact that design freezes are most consequential when no further adjustment is available after the freeze. The optimal values of the decision variables identified

through the co-design optimization are shown in Table 2. Even when considering model uncertainty, by adding plant and controller adaptability, the expected value of the system's net profit increases by over $1.1MM as compared to a system optimized based on a perfect model (negating time costs) with zero adaptability and by over $1.7MM as compared to a system optimized based on an uncertain model with zero adaptability.

Table 2. Optimal co-design parameters

Variable	Description	Value	Units
r_b^*	Optimal blade length	116.3	m
TSR^*	Optimal TSR setpoint	8.20	$(-)$
Δ_β^*	Optimal coning range	20	$^\circ$
K_{type}^*	Optimal control strategy	1	$(-)$
t_p^*	Optimal plant freeze date	3	months
t_c^*	Optimal controller freeze date	3	months

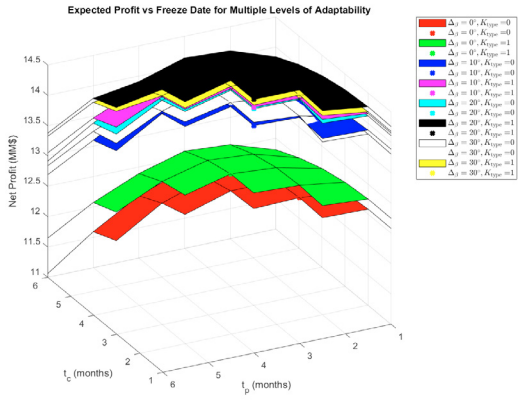

Fig. 5. Expected lifetime profit of SUMR systems with multiple levels of plant and controller adaptability vs freeze date. The profit-optimal freeze date for each design is indicated with an X on each surface.

4. REAL-TIME ADAPTIVE DESIGN REALIZATION

This section describes the underlying adaptive controller that realizes the adaptation made possible through the aforementioned co-design process.

4.1 Dynamic Model

The dynamic model used for analysis and control design has been adopted from P. J. Moriarty (2005) and is given by:

$$\dot{\omega} = \frac{\tau_{\text{aero}} - \tau_{\text{gen}}}{I_{\text{base}} \cos^2(\beta)} \tag{18}$$

where ω is the rotor speed, I_{base} is the turbine's unconed moment of inertia, and τ_{gen} is the applied generator torque. The plant model has three control input channels, τ_{gen}, β, and θ. Here, τ_{gen} directly influences the system dynamics in Eqn. 18, while β and θ impact the system dynamics through their effects on the moment of inertia and aerodynamic torque.

4.2 Real-Time Control Implementation

Feedback Controller: By solving the optimization problem described in Sec. 3.2.2 in the absence of uncertainty (reflecting model knowledge at the time of deployment) offline, lookup tables were generated that recorded the power-optimal, constraint-satisfying TSR, coning angle, and blade pitch for a given wind speed. A constant-gain PI controller was applied to the error between the current TSR and the lookup table's optimal TSR setpoint to compute the generator torque necessary to achieve the desired TSR setpoint. This PI controller was formulated as:

$$\tau_{\text{gen}} = k_{P,\tau}(TSR - TSR_{\text{SP}}) + k_{I,\tau} \int_0^t (TSR - TSR_{\text{SP}}) d\bar{t} \tag{19}$$

where $k_{P,\tau}$ is a proportional gain, $k_{I,\tau}$ is an integral gain, and TSR_{SP} is the tip-speed-ratio setpoint retrieved from the lookup table. Further, Eqn. 19 can be simplified by defining the TSR wind speed lookup table as $TSR_{\text{SP}} = f(v_w)$. Substituting this expression into Eqn. 19, the torque control law becomes dependent only on the TSR and wind speed.

The gain-scheduled PI pitch controller described in Zalkind et al. (2017) ensured constraint satisfaction in the event of model mismatch between the quasi-static and dynamic models.

4.3 Dynamic Simulation

Dynamic simulations were conducted using the dynamic model described in Sec. 4.1 to demonstrate the practical implementation of a real-time control strategy developed using this co-design approach. The performance of a SUMR turbine utilizing the feedback control strategy from Sec. 4.2.1 was simulated over 24 hours. The wind speed profile was based on time series data at the installation site as plotted in Fig. 6.

As shown in Figs. 7 and 8, the proposed strategy (that fully leverages the system's capacity for adaptation) enabled the system to operate at high wind speeds without violating the constraints of maximum mechanical power generation or maximal allowable bending load. In Fig. 7, energy and power generation predicted by the quasi-static model (described in 3.2.2) are shown to exceed the power generation calculated by the dynamic simulation model by less than 0.5%, demonstrating that the impact of transient tracking behavior in the proposed control strategy is very small. The controller enabled the turbine to maintain loading at the structural constraint over a wide range of wind speeds by increasing generator torque, reducing the coning angle, and increasing the blade pitch angle as shown by the control trajectories plotted in Fig. 6.

5. CONCLUSIONS

In this work, an adaptability-aware control co-design framework was presented. This framework was then applied to the SUMR using quasi-static models for performance, which were later validated via dynamic simulation. Through this co-design process, the lifetime-profit-optimal blade length, tip-speed-ratio setpoint, range of cone angle adjustment, control strategy, and freeze dates were selected. The design optimized while considering adaptation was projected to have a lifetime profit 6.5% greater than a system developed without considering real-time adaptation. A simple feedback control strategy was developed to leverage the system's adaptability, which was validated in a dynamic simulation framework. This work serves as an initial validation of the proposed co-design framework that has the potential to increase the profitability of renewable energy systems, incentivizing widespread adoption of sustainable energy.

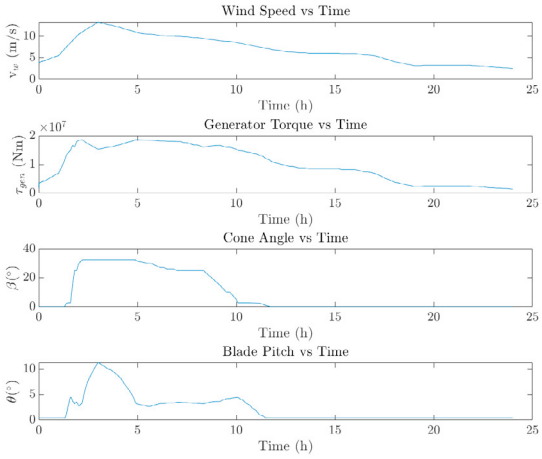

Fig. 6. Wind speed, generator torque, cone angle, and blade pitch vs time over 24-hour simulation.

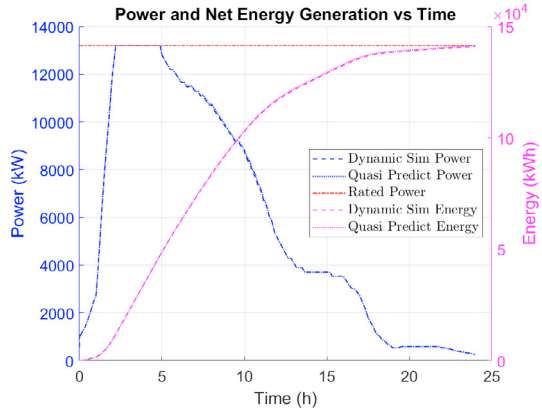

Fig. 7. Power and energy generation vs time over 24-hour simulation and a quasi-static prediction under perfect tracking.

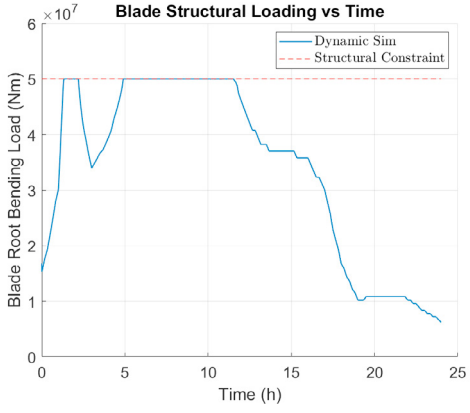

Fig. 8. Root bending moment vs time over 24-hour simulation.

REFERENCES

Ananda, G., Bansal, S., and Selig, M. (2018). Aerodynamic design of a 13.2 mw segmented ultralight morphing rotor. doi:10.2514/6.2018-0994.

Bayat, S., Lee, Y.H., and Allison, J.T. (2023). Nested control co-design of a spar buoy horizontal-axis floating offshore wind turbine. doi:10.48550/arXiv.2310.15463.

Fine, J.B., McGuire, C.M., Reed, J., Bryant, M., and Vermillion, C. (2023). Optimal cyclic control of a structurally constrained span-morphing underwater kite in a spatiotemporally varying flow. In *2023 American Control Conference (ACC)*, 2084–2090. doi:10.23919/ACC55779.2023.10155864.

Fine, J.B., Reed, J., Naik, K., and Vermillion, C. (2022). Predictive control of a morphing energy-harvesting kite. In *2022 IEEE Conference on Control Technology and Applications (CCTA)*, 1246–1252. doi:10.1109/CCTA49430.2022.9966031.

Holtberg, P.D. et al. (2011). *Annual Energy Outlook 2011: With Projections to 2035*. Government Printing Office.

Kianbakht, S., Martin, D., Johnson, K., Zalkind, D., Pao, L., Loth, E., Simpson, J., Yao, S., Chetan, M., and Griffith, D. (2022). Design space exploration and decision-making for a segmented ultralight morphing 50-mw wind turbine. *Wind Energy*, 25, n/a–n/a. doi:10.1002/we.2781.

L. Fingersh, M.H. and Laxson, A. (2006). Wind turbine design cost and scaling model : Nrel/tp-500-40566. Technical report, NREL.

Lantz, E., Sigrin, B., Gleason, M., Preus, R., and Baring-Gould, I. (2016). Assessing the future of distributed wind: Nrel/tp-6a20-67337. Technical report, NREL.

Naik, K. and Vermillion, C. (2024). Integrated physical design, control design, and site selection for an underwater energy-harvesting kite system. *Renewable Energy*, 220, 119687. doi:https://doi.org/10.1016/j.renene.2023.119687.

Noyes, C., Loth, E., Martin, D., Johnson, K., Ananda, G., and Selig, M. (2020). Extreme-scale load-aligning rotor: To hinge or not to hinge? *Applied Energy*, 257, 113985. doi:https://doi.org/10.1016/j.apenergy.2019.113985.

P. J. Moriarty, A.C.H. (2005). Aerodyn theory manual: Nrel/tp-500-36881. Technical report, NREL.

Pao, L.Y., Pusch, M., and Zalkind, D.S. (2023). Control co-design of wind turbines. *Annual Review of Control, Robotics, and Autonomous Systems*. doi:https://doi.org/10.1146/annurev-control-061423-101708.

Roberto Lacal-Arántegui, José M. Yustab, J.A.D.N. (2018). Offshore wind installation: Analysing the evidence behind improvements in installation time. *Renewable and Sustainable Energy Reviews*, 92, 133–145.

Rotea, M.A. (2017). Logarithmic power feedback for extremum seeking control of wind turbines. *IFAC-PapersOnLine*, 50(1), 4504–4509. doi:https://doi.org/10.1016/j.ifacol.2017.08.381. 20th IFAC World Congress.

Sengupta, M., Xie, Y., Lopez, A., Habte, A., Maclaurin, G., and Shelby, J. (2018). The national solar radiation data base (nsrdb). *Renewable and Sustainable Energy Reviews*, 89. doi:10.1016/j.rser.2018.03.003.

Wiser, R.H. and Bolinger, M. (2019). 2018 wind technologies market report.

Zalkind, D., Pao, L., Martin, D., and Johnson, K. (2017). Models used for the simulation and control of a segmented ultralight morphing rotor. *IFAC-PapersOnLine*, 50, 4478–4483. doi:10.1016/j.ifacol.2017.08.377.